Mechanism of microtubule plus-end tracking by the plant-specific SPR1 protein and its development as a versatile plus-end marker

Received for publication, April 12, 2019, and in revised form, September 12, 2019 Published, Papers in Press, September 16, 2019, DOI 10.1074/jbc.RA119.008866

Rachappa Balkunde[‡], Layla Foroughi[‡], Eric Ewan[§], Ryan Emenecker[‡], Valeria Cavalli[§¶‖], and Ram Dixit[‡1]

From the [‡]Department of Biology and Center for Engineering Mechanobiology, Washington University, St. Louis, Missouri 63130 and the [§]Department of Neuroscience, [¶]Center of Regenerative Medicine, and [‖]Hope Center for Neurological Disorders, Washington University School of Medicine, St. Louis, Missouri 63110

Edited by Enrique M. De La Cruz

Microtubules are cytoskeletal polymers that perform diverse cellular functions. The plus ends of microtubules promote polymer assembly and disassembly and connect the microtubule tips to other cellular structures. The dynamics and functions of microtubule plus ends are governed by microtubule plus end–tracking proteins (+TIPs). Here we report that the *Arabidopsis thaliana* SPIRAL1 (SPR1) protein, which regulates directional cell expansion, is an autonomous +TIP. Using *in vitro* reconstitution experiments and total internal reflection fluorescence microscopy, we demonstrate that the conserved N-terminal region of SPR1 and its GGG motif are necessary for +TIP activity whereas the conserved C-terminal region and its PGGG motif are not. We further show that the N- and C-terminal regions, either separated or when fused in tandem (NC), are sufficient for +TIP activity and do not significantly perturb microtubule plus-end dynamics compared with full-length SPR1. We also found that exogenously expressed SPR1-GFP and NC-GFP label microtubule plus ends in plant and animal cells. These results establish SPR1 as a new type of intrinsic +TIP and reveal the utility of NC-GFP as a versatile microtubule plus-end marker.

Microtubules are dynamic polymers of $\alpha\beta$-tubulin heterodimers and form different arrays to orchestrate critical cellular activities in eukaryotes. The plus ends of microtubules are of particular significance because they drive the assembly and disassembly of microtubules and connect microtubule tips to various cellular structures. Specialized proteins called microtubule plus end–tracking proteins (+TIPs)[2] specifically accumulate at growing microtubule plus ends and control their behavior and interactions. +TIPs can directly or indirectly target growing microtubule plus ends (1). For example, the evolutionarily conserved end binding (EB) proteins autonomously target growing microtubule plus ends by recognizing GDP/P_i-tubulin structures (2–7). In turn, EBs recruit a host of other proteins as part of a dynamically changing microtubule plus-end complex (8, 9).

Land plants contain a unique set of +TIPs (10–12), perhaps because they assemble morphologically and functionally distinct microtubule arrays compared with animals (13). One of the plant-specific +TIPs is the *Arabidopsis thaliana* SPIRAL1 (SPR1) protein. *SPR1* was identified through a genetic screen for skewed root growth (14) and encodes a 12-kDa protein that localizes to the growing plus end of cortical microtubules and contributes to anisotropic cell expansion (11, 12, 15). SPR1 genetically and physically interacts with the *A. thaliana* END BINDING 1b (EB1b) protein (16), which tracks growing microtubule plus ends, similar to animal and yeast EB proteins (17, 18). However, SPR1 is also able to bind to free tubulin and the microtubule lattice independently of EB1b *in vitro* (16), raising the question of whether SPR1 needs EB1b for microtubule plus-end localization. Here we report that SPR1 is an autonomous +TIP and identify the regions and critical residues that are required for this activity. Finally, we show that a fusion protein consisting of the conserved N- and C-terminal regions of SPR1 fused to GFP labels growing microtubule plus ends in plant and animal cells, making it a versatile microtubule plus-end marker.

Results

SPR1 is an autonomous microtubule plus end–tracking protein

To study the mechanism of SPR1's +TIP activity, we took an *in vitro* reconstitution approach with purified recombinant SPR1-GFP protein (Fig. 1*A*) and dynamic microtubules using porcine tubulin. We found that SPR1-GFP on its own labels microtubule plus ends exclusively during the growth phase (Fig. 1, *B* and *C*, and Movie S1). We observed that SPR1-GFP also weakly labels growing microtubule minus ends (Fig. 1*C* and Movie S1), similar to yeast and mammalian EB proteins (2, 3). Furthermore, SPR1-GFP expressed under its native promoter labels microtubule plus ends in the *eb1a;eb1b* double mutant (Fig. 1*D*), demonstrating that SPR1 does not require EB1a and EB1b to localize to microtubule plus ends *in vivo*.

Funding was provided by NINDS, National Institute of Health Grant R01 NS082446 (to V. C.) and National Science Foundation CAREER Program Grant 1453726 and NIGMS, National Institute of Health Grant R01 GM114678 (to R. D.). The authors declare that they have no conflicts of interest with the contents of this article. The content is solely the responsibility of the authors and does not necessarily represent the official views of the National Institutes of Health.

This article contains Figs. S1 and S2, Table S1, and Movies S1–S5.

[1] To whom correspondence should be addressed. Tel.: 314-935-8823; Fax: 314-935-4432; E-mail: ramdixit@wustl.edu.

[2] The abbreviations used are: +TIP, microtubule plus end–tracking protein; EB, end binding; GTPγS, guanosine 5′-3-*O*-(thio)triphosphate; GMPCPP, guanosine-5′-[($\alpha\beta$)-methyleno] triphosphate; EGFP, enhanced GFP; mW, milliwatt; ANOVA, analysis of variance; RFP, red fluorescent protein.

© 2019 Balkunde et al. Published under exclusive license by The American Society for Biochemistry and Molecular Biology, Inc.

Downloaded from http://www.jbc.org/ at Washington University on November 1, 2019

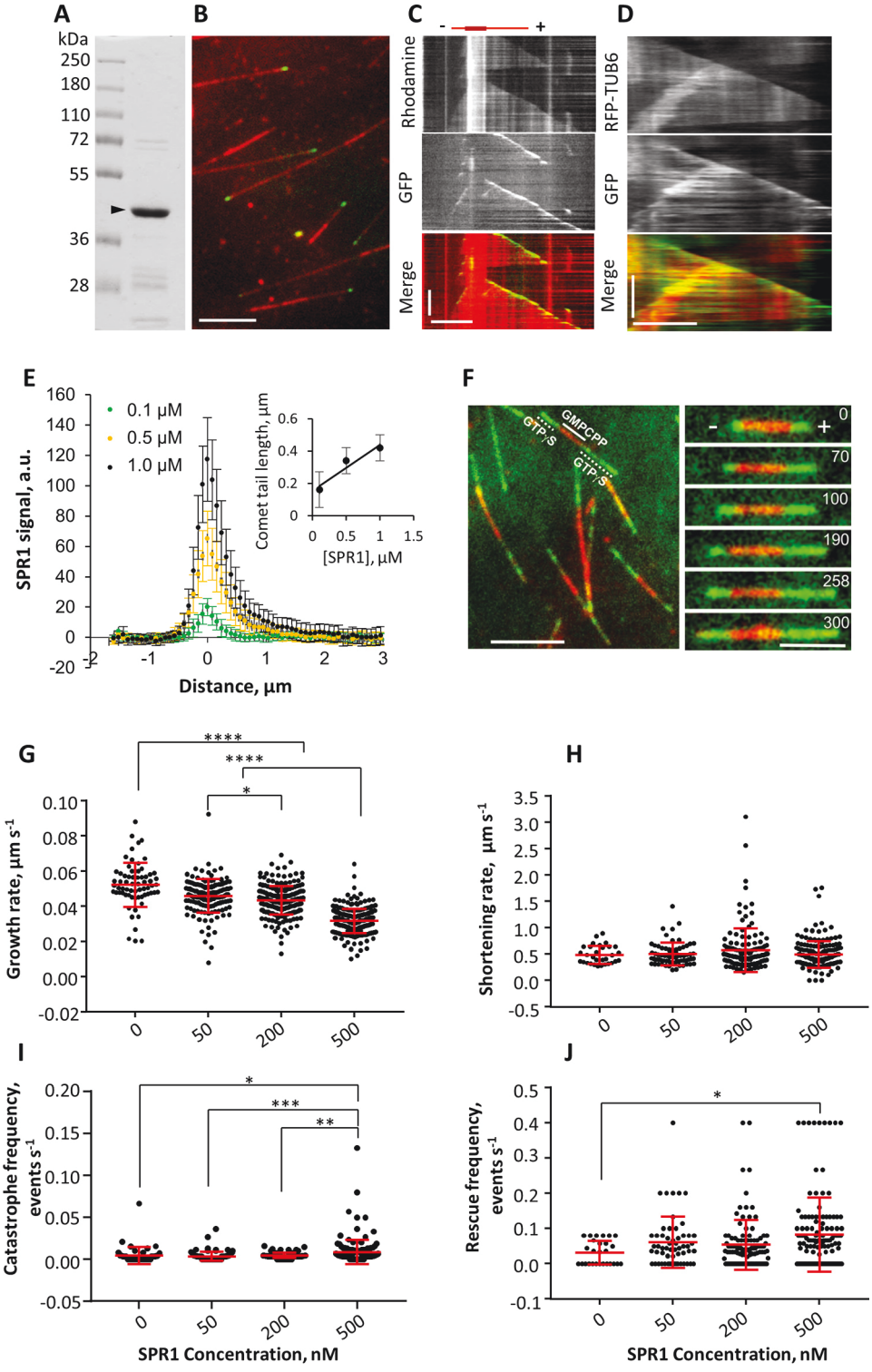

Figure 1. SPR1 is an autonomous microtubule plus end–tracking protein. *A*, Coomassie-stained gel of recombinant SPR1-GFP protein. The *arrowhead* indicates the expected size (40 kDa) of the protein. Numbers on the *left* indicate the size of the protein bands in the ladder. *B*, representative image of SPR1-GFP (*green*) and dynamic rhodamine-labeled microtubules (*red*). *Scale bar* = 5 μm. *C*, representative kymograph of SPR1-GFP (*green*) and a dynamic rhodamine-labeled microtubule (*red*). *x axis scale bar* = 5 μm, *y axis scale bar* = 100 s. *D*, representative kymograph of SPR1-GFP (*green*) and RFP-TUB6 (*red*) in the *eb1a;eb1b* double mutant. *x axis scale bar* = 5 μm, *y axis scale bar* = 100 s. *E*, graph of SPR1-GFP signal intensity at the plus end of growing microtubules *in vitro*. Values represent mean ± S.D. $n = 52$, 89, and 133 for 0.1 μM, 0.5 μM, and 1 μM SPR1-GFP, respectively. *Inset*, the length of the comet tail as a function of SPR1-GFP concentration. Comet tail lengths were obtained by fitting the right halves of the signal intensity curves to single exponentials. *a.u.*, arbitrary units. *F*, representative image of SPR1-GFP (*green*) bound to GTPγS microtubules grown from GMPCPP microtubule seeds (*red*). The montage on the *right* shows an example of a growing GTPγS microtubule being bound by SPR1-GFP. *Scale bars* = 5 μm. *G–J*, dot plots of microtubule growth rate (*G*), shortening rate (*H*), catastrophe frequency (*I*), and rescue frequency (*J*) at the indicated SPR1-GFP concentrations. Statistical analyses were conducted using one-way ANOVA. ****, $p < 0.0001$; ***, $p < 0.001$; **, $p < 0.01$; *, $p < 0.05$.

Downloaded from http://www.jbc.org/ at Washington University on November 1, 2019

The SPR1-GFP signal is concentrated at the tips of growing microtubules and decays exponentially along the microtubule lattice in a comet-like pattern (Fig. 1, *B* and *E*). Increasing the concentration of SPR1-GFP protein enhanced the accumulation of SPR1 at the tips of growing microtubule plus ends and increased the length of the comet tails along the microtubule lattice (Fig. 1*E*). Human EB1 has been reported to result in either an increase (3) or decrease (6) in comet size with increasing EB1 concentration. To determine whether the plus end–tracking activity of SPR1 involves recognition of the nucleotide state of tubulin, we examined the binding of SPR1 to microtubules polymerized in the presence of the GTP analog guanosine 5′-3-*O*-(thio)triphosphate (GTPγS), which mimics the structure of growing microtubule ends (4–7). We found that SPR1-GFP preferentially binds to the GTPγS microtubule lattice compared with the guanosine-5′-[(αβ)-methyleno] triphosphate (GMPCPP) microtubule seeds (Fig. 1*F*). These data suggest that the SPR1 and EB proteins share a similar mechanism for recognizing growing microtubule ends.

To determine whether SPR1-GFP affects the behavior of microtubule plus-ends *in vitro*, we measured the dynamic instability parameters at various SPR1-GFP concentrations. We observed that SPR1-GFP inhibited the growth rate of microtubule plus ends and enhanced their catastrophe frequency in a concentration-dependent manner (Fig. 1, *G* and *I*). In contrast, SPR1-GFP did not significantly affect the shortening rate of microtubule plus ends and only modestly increased their rescue frequency at the highest SPR1-GFP concentration tested (Fig. 1, *H* and *J*). These observations (summarized in Table S1) are largely consistent with the reported changes in microtubule plus-end dynamics in *spr1* loss-of-function mutants compared with the WT (19).

The conserved N-terminal region is the primary determinant of SPR1's +TIP activity

SPR1 is the smallest known +TIP; therefore, we wanted to identify the regions that confer microtubule plus-end localization. The conserved N- and C-terminal regions of SPR1 (Fig. 2*A*) have been proposed to contribute to microtubule binding because they contain a GGG and a PGGG motif, respectively, which are part of the microtubule-binding repeats of the MAP2/tau family of microtubule-associated proteins (11, 12).

To determine the relative contribution of the N- and C-terminal regions of SPR1, we created truncated versions of SPR1 that lacked either the N-terminal or the C-terminal regions (Fig. 2, *B* and *C*). We found that deleting the N-terminal 18 amino acids (SPR1Δ1–18) abolished +TIP activity *in vitro* (Fig. 2*D*), indicating that the N-terminal region of SPR1 is essential for recognizing the microtubule plus end. Deletion of the C-terminal 33 amino acids (SPR1Δ87–119) diminished the signal at growing microtubule plus ends but did not eliminate it (Fig. 2*D*), indicating that the C-terminal region enhances the +TIP activity of SPR1 but is not necessary for it. Consistent with these findings and with previous *in vivo* work (11), the chimeric N-GFP-C protein clearly localized to growing microtubule plus ends *in vitro* (Fig. 2*D* and Movie S2). To test whether the spacing of the N- and C-terminal regions is important for +TIP activity, we fused these regions in tandem to GFP (Fig. 2, *B* and *C*). The resulting NC-GFP fusion protein also localized to growing microtubule plus ends *in vitro* (Fig. 2*D* and Movie S3).

During these experiments, we noticed that the microtubule plus-end signals of N-GFP-C and NC-GFP were less than the SPR1-GFP signal. To determine whether the N-GFP-C and NC-GFP proteins have a lower affinity for the microtubule plus end compared with SPR1-GFP, we conducted *in vitro* dynamic microtubule assays under single-molecule imaging conditions followed by kymograph analysis (Fig. 2*F*). Photobleaching experiments revealed that the majority of SPR1-GFP particles were monomeric (97.7% monomers, 2.3% dimers, $n = 175$). Similarly, the majority of N-GFP-C and NC-GFP particles were also monomeric (92% monomers, 8% dimers, $n = 88$ for N-GFP-C; 91.2% monomers, 8.8% dimers, $n = 158$ for NC-GFP). We measured the binding rate and dwell time of individual particles to calculate the binding rate constant (k_{on}) and unbinding rate constant (k_{off}) of SPR1-GFP, N-GFP-C, and NC-GFP for the growing microtubule plus end. Our findings showed that N-GFP-C and NC-GFP bind more weakly to microtubule plus ends compared with SPR1-GFP (Fig. 2*G*).

Next we tested the significance of the N-terminal GGG and C-terminal PGGG motifs by mutating these amino acids to alanine within the context of full-length SPR1 (Fig. 2, *B* and *C*). Although mutation of PGGG to AAAA ($SPR1^{PGGG\text{-}AAAA}$) had no effect on the +TIP activity of SPR1, mutation of GGG to AAA ($SPR1^{GGG\text{-}AAA}$) abolished this activity (Fig. 2*E*). These findings underscore the essential role of the SPR1 N-terminal region and indicate that the GGG motif in the N-terminal region is critical for +TIP activity.

The N-GFP-C and NC-GFP markers do not significantly alter microtubule dynamics

The autonomous +TIP activity of N-GFP-C and NC-GFP makes them attractive microtubule plus-end markers. To determine whether they affect microtubule plus-end dynamics similar to the WT SPR1 protein, we tested the effect of N-GFP-C and NC-GFP on microtubule dynamics *in vitro*. We found that N-GFP-C did not significantly alter the microtubule growth rate (Fig. 3*A*), catastrophe frequency (Fig. 3*C*), or rescue frequency (Fig. 3*D*) and only modestly increased the shortening rate (Fig. 3*B*). NC-GFP did not significantly alter any of these microtubule dynamic instability parameters (Fig. 3, *E–H*, and Table S1). Furthermore, we compared the number of growth-to-shortening and shortening-to-growth transition events exhibited by individual microtubules at different concentrations of SPR1-GFP, N-GFP-C, and NC-GFP. We found that SPR1-GFP boosted microtubule transitions in a concentration-dependent manner (Fig. 3*I*), consistent with its enhancement of catastrophe and rescue frequencies (Fig. 1, *I* and *J*). In contrast, neither N-GFP-C nor NC-GFP significantly altered the number of microtubule transitions (Fig. 3, *J* and *K*). Taken together, our findings demonstrate that N-GFP-C and NC-GFP localize to growing microtubule plus ends without significantly perturbing their dynamics, unlike WT SPR1.

Downloaded from http://www.jbc.org/ at Washington University on November 1, 2019

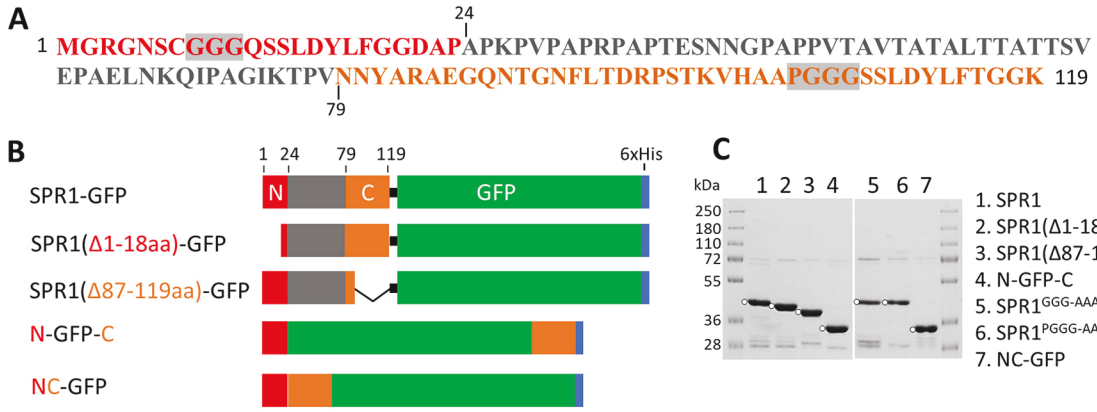

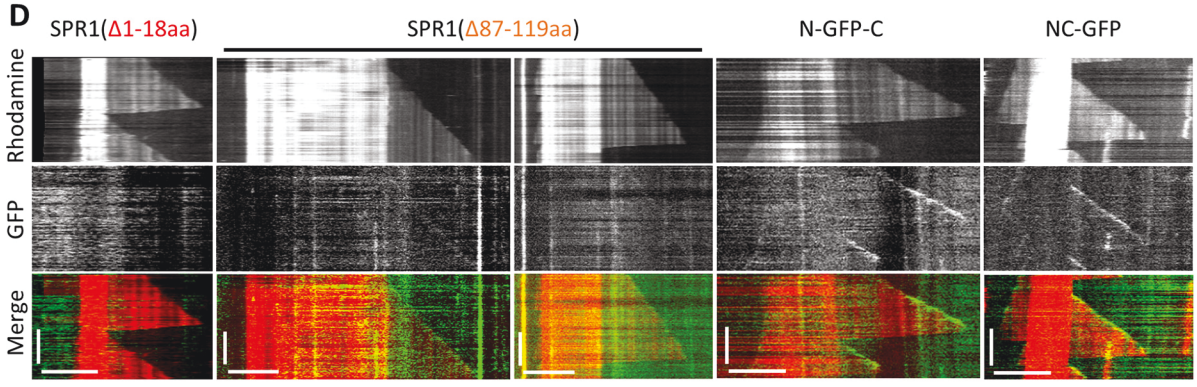

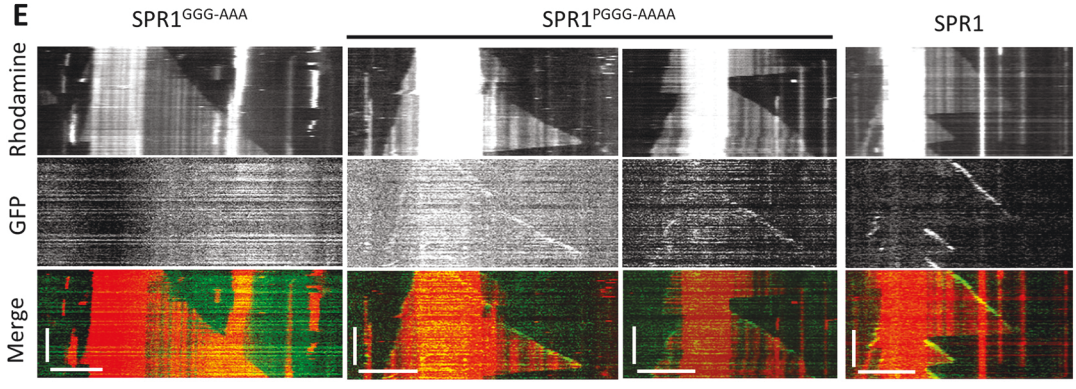

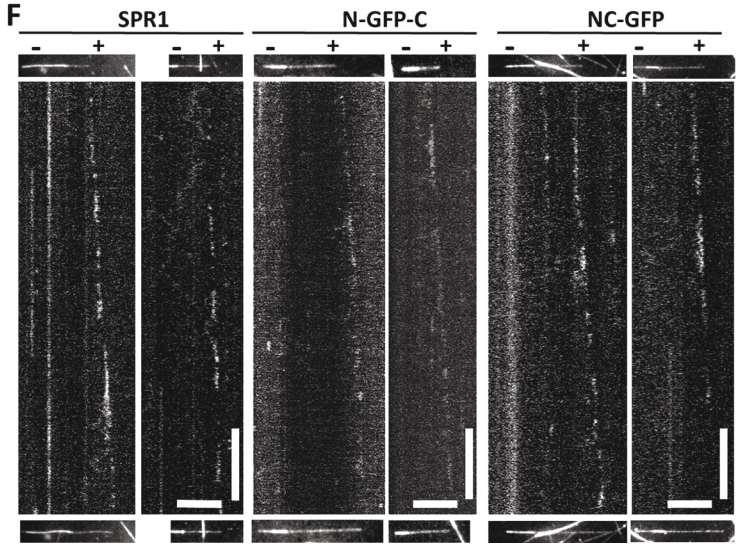

G

	SPR1	N-GFP-C	NC-GFP
k_{on} $\mu M^{-1}.\mu m^{-1}.s^{-1}$	0.41 ± 0.41 (n = 93)	0.1 ± 0.05 (n = 69)	0.27 ± 0.15 (n = 64)
k_{off} s^{-1}	0.36 ± 0.01 (n = 488)	0.28 ± 0.02 (n = 294)	0.55 ± 0.03 (n = 459)
K_D $\mu M.\mu m$	0.87	2.8	2.03

Downloaded from http://www.jbc.org/ at Washington University on November 1, 2019

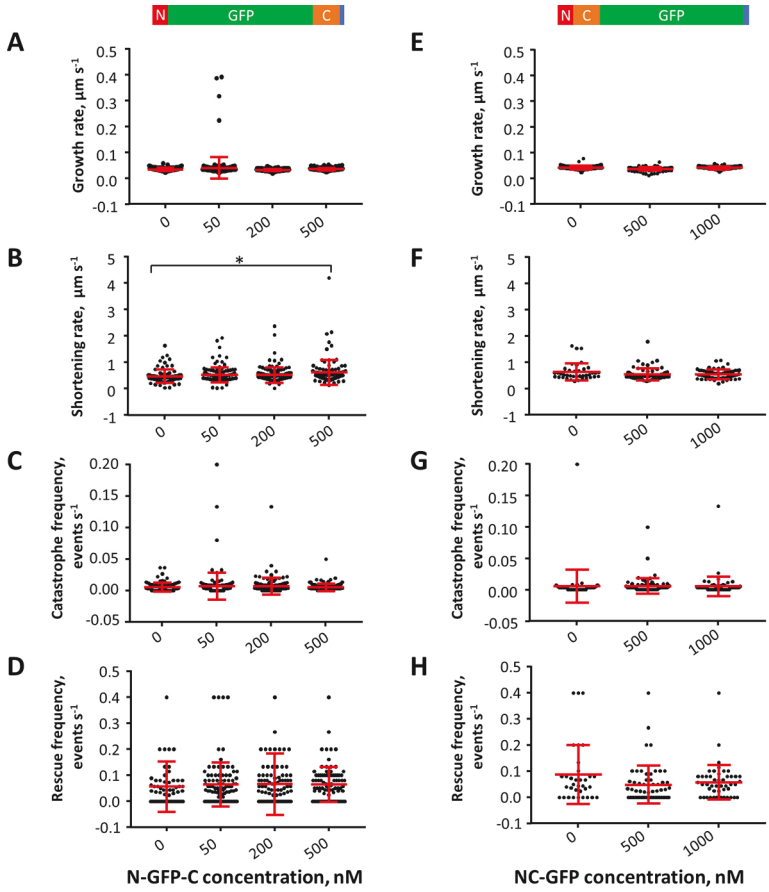

I SPR1-GFP

[protein], nM	0	50	200	500
# Transitions >2	8	12	19	25
2	17	31	35	28
1	26	15	22	28
0	49	42	24	19
N	53	100	140	158

J N-GFP-C

0	50	200	500
16	12	15	17
19	33	25	32
25	23	31	26
40	32	29	25
108	144	134	118

K NC-GFP

0	500	1000
10	15	13
31	30	33
14	21	15
45	34	39
108	144	134

Figure 3. N-GFP-C and NC-GFP do not significantly affect microtubule dynamics *in vitro*. *A–D*, dot plots of microtubule growth rate (*A*), shortening rate (*B*), catastrophe frequency (*C*), and rescue frequency (*D*) at the indicated N-GFP-C protein concentrations. *, $p < 0.05$; one-way ANOVA. *E–H*, dot plots of microtubule growth rate (*E*), shortening rate (*F*), catastrophe frequency (*G*), and rescue frequency (*H*) at the indicated NC-GFP protein concentrations. *I–K*, the percentage of microtubule transition events (*i.e.* switch from growth to shortening or from shortening to growth) at increasing concentrations of SPR1-GFP (*I*), N-GFP-C (*J*), and NC-GFP (*K*). *Numbers* are the percentages of each category of microtubule transitions during the observation period.

NC-GFP labels growing microtubule plus ends in plants and partially complements the spr1 mutant phenotype

To determine whether *NC-GFP* is functional *in vivo*, we expressed it under the constitutive *A. thaliana UBIQUITIN10 (pUBQ10)* promoter in *spr1–6* mutant plants. *pUBQ10:SPR1-GFP* and *pUBQ10:N-GFP-C* constructs were included as controls. All three constructs were also expressed in WT plants expressing an RFP-TUB6 microtubule marker to determine their microtubule localization in plants.

We found that SPR1-GFP fully complements the hypocotyl cell file skewing phenotype of the *spr1–6* mutant, whereas the NC-GFP and N-GFP-C constructs only partially complemented this phenotype (Fig. 4, *A* and *B*). Our data for SPR1-GFP and N-GFP-C are consistent with previous work that

Figure 2. The N-terminal region of SPR1 is required for microtubule plus-end tracking. *A*, SPR1 amino acid sequence. The conserved N-terminal and C-terminal regions are shown in *red* and *orange*, respectively. The central variable region is shown in *gray*. *Gray boxes* indicate the conserved GGG and PGGG motifs in the N-terminal and C-terminal regions, respectively. *B*, schematic of the full-length SPR1-GFP fusion protein and mutant SPR1 proteins used in this study. The color code is the same as in *A*. *C*, Coomassie-stained gel of the truncated and chimeric versions of SPR1 protein used in this study. *White dots* indicate the expected protein bands. *D*, representative kymographs of SPR1(Δ1–18)-GFP, SPR1(Δ87–119)-GFP, N-GFP-C, and NC-GFP proteins. *x axis scale bar* = 5 μm, *y axis scale bar* = 100 s. *E*, representative kymographs of $SPR1^{GGG\text{-}AAA}$-GFP and $SPR1^{PGGG\text{-}AAAA}$-GFP proteins. A kymograph of WT SPR1-GFP is shown for comparison. *x axis scale bar* = 5 μm, *y axis scale bar* = 100 s. *F*, representative kymographs from single-molecule imaging experiments of SPR1-GFP, N-GFP-C, and NC-GFP proteins. Images at the *top* and *bottom* of the kymographs show the microtubule at the beginning and at the end of streaming-mode image acquisition. *x axis scale bar* = 5 μm, *y axis scale bar* = 10 s. *G*, table of the k_{on}, k_{off}, and apparent K_D of SPR1-GFP, N-GFP-C, and NC-GFP proteins. Values are mean ± S.D. (*n* = number of molecules).

Downloaded from http://www.jbc.org/ at Washington University on November 1, 2019

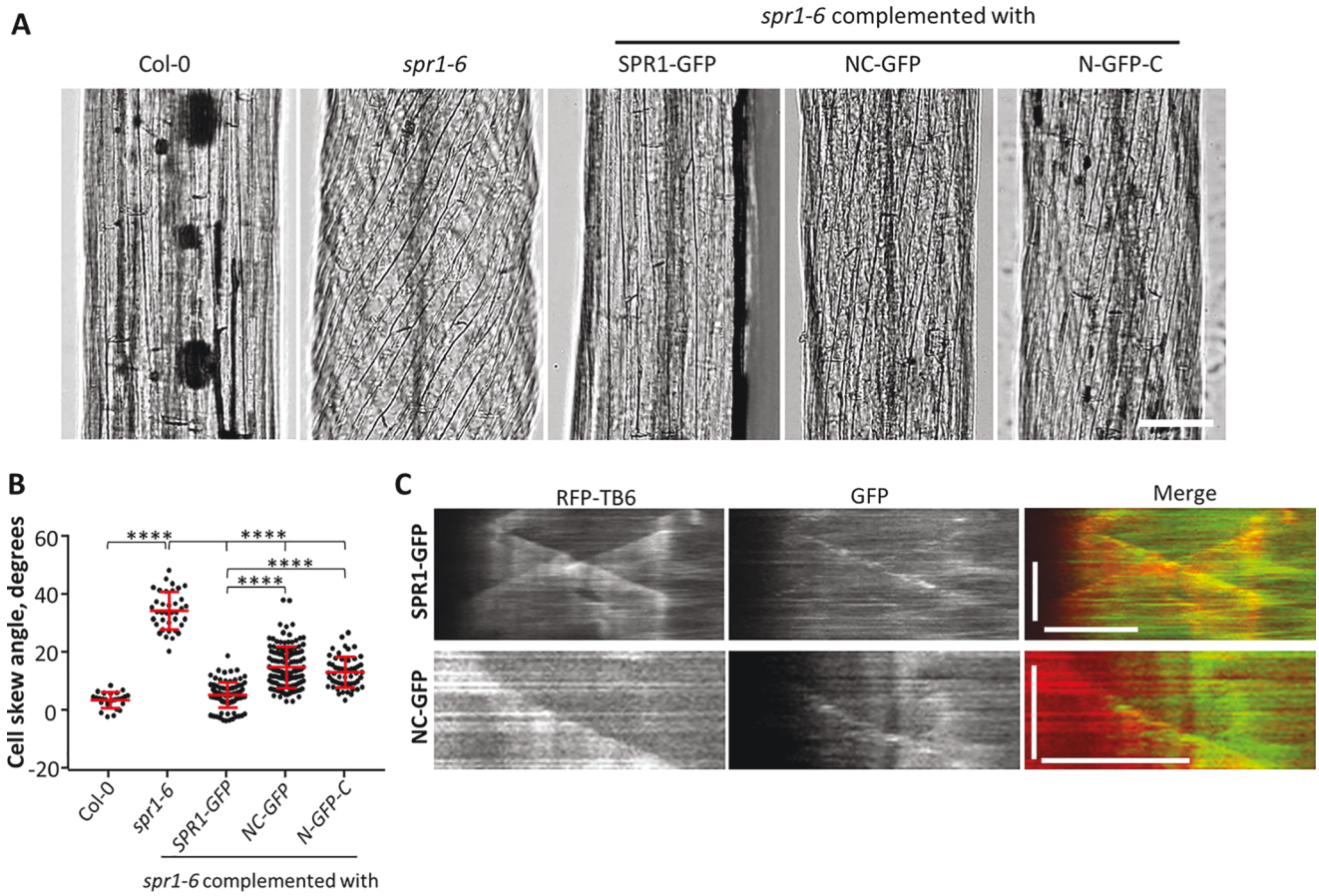

Figure 4. NC-GFP labels growing microtubule plus ends in plants. *A*, bright-field images of dark-grown hypocotyls of Col-0, spr1–6 mutant, and spr1–6 mutant expressing either SPR1-GFP, NC-GFP, or N-GFP-C. *Scale bar* = 100 μm. *B*, dot plot of the orientation of cells with respect to the hypocotyl growth axis. One-way ANOVA; ****, $p < 0.0001$; $n = 26$, 37, 67, 123, and 53 cells for Col-0, spr1–6, SPR1-GFP, NC-GFP, and N-GFP-C plants, respectively. *C*, representative kymographs of SPR1-GFP and NC-GFP expressed in WT *Arabidopsis* plants expressing an RFP-TUB6 microtubule marker. *x axis scale bar* = 5 μm, *y axis scale bar* = 100 s.

expressed these constructs under a cauliflower mosaic virus 35S promoter and reported complete and partial complementation of root skewing in *spr1–6*, respectively (11). Notably, although the N-GFP-C signal was barely above our detection threshold, NC-GFP localized to growing microtubule plus ends *in vivo* (Fig. 4*C*). These observations indicate that NC-GFP can be used as a microtubule plus-end marker in plants. We also found that NC-GFP preferentially binds to GTPγS microtubules, similar to SPR1-GFP (Fig. S1), indicating that NC-GFP also recognizes GDP/P_i-tubulin at growing microtubule plus ends.

SPR1-GFP and NC-GFP label growing microtubule plus ends in animal cells

Because SPR1-GFP, N-GFP-C, and NC-GFP labeled the plus ends of microtubules assembled from porcine tubulin *in vitro*, we reasoned that they might label microtubule plus ends in animal cells. To test the suitability of these proteins as microtubule plus-end markers in animal cells, we introduced them in HEK293 cells and imaged the transfected cells using total internal reflection fluorescence microscopy. GFP-labeled human tubulin and EB3 were included as controls in these experiments. As expected, GFP-tubulin labeled the entire microtubule lattice, whereas EB3-GFP localized to growing microtubule plus ends (Fig. 5, *A* and *B*). Interestingly, both SPR1-GFP and NC-GFP clearly labeled growing microtubule plus ends and the microtubule shaft to a lesser extent (Fig. 5, *C* and *D*, and Movies S4 and S5). To assess whether SPR1-GFP and NC-GFP affect microtubule dynamics in HEK293 cells, we quantified microtubule growth rates in cells expressing these proteins (Fig. 5*E*). Cells expressing SPR1-GFP had slightly higher microtubule growth rates (0.23 ± 0.07 μm/s, $n = 105$ microtubules) compared with cells expressing GFP-tubulin (0.17 ± 0.06 μm/s, $n = 114$ microtubules) or EB3-GFP (0.17 ± 0.07 μm/s, $n = 105$ microtubules). Expression of NC-GFP in HEK293 cells had a less pronounced effect on the microtubule growth rate (0.19 ± 0.04 μm/s, $n = 99$ microtubules) compared with SPR1-GFP. Importantly, SPR1-GFP and NC-GFP did not visibly impair the viability and morphology of HEK293 cells (Fig. S2), indicating that these proteins are not toxic to animal cells. Although N-GFP-C showed an extensive cytoplasmic signal in HEK293 cells, we were unable to detect unambiguous microtubule plus-end labeling.

Discussion

We demonstrate that the 12-kDa plant-specific *Arabidopsis* SPR1 protein is an autonomous microtubule plus end–tracking protein. Using truncations and mutations in SPR1, we reveal

Downloaded from http://www.jbc.org/ at Washington University on November 1, 2019

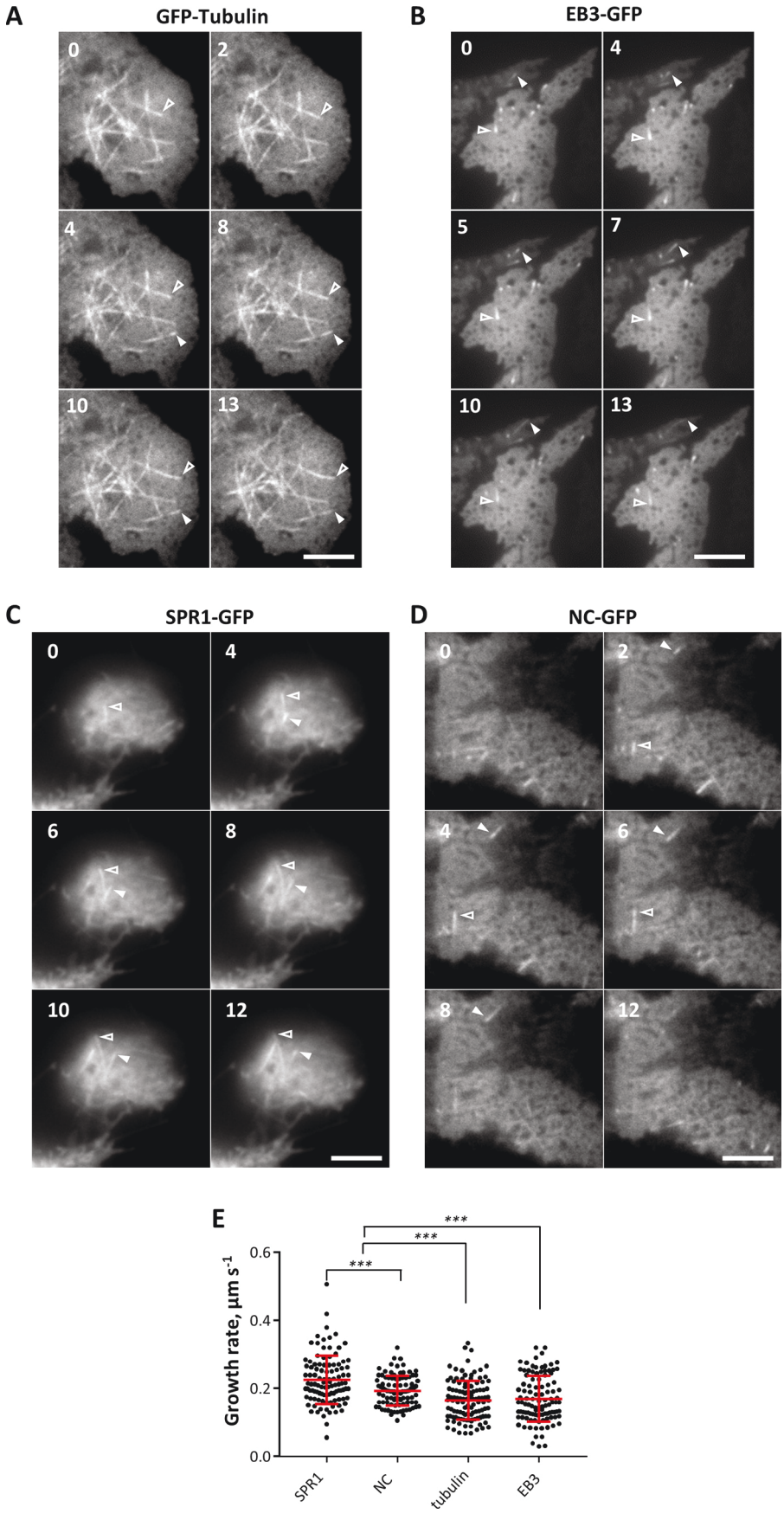

Downloaded from http://www.jbc.org/ at Washington University on November 1, 2019

that the conserved N-terminal region and its GGG motif are critical for plus end–tracking activity, whereas the conserved C-terminal region and its PGGG motif are dispensable. Our GTPγS microtubule binding experiments showed that SPR1 targets growing microtubule ends by recognizing the GDP/P_i state of tubulin, similar to EB proteins. However, SPR1 does not share any sequence similarity with EBs or other known +TIPs. Therefore, our findings establish a new category of intrinsic +TIPs unique to plants.

Because both SPR1 and EB1 proteins recognize the GDP/P_i tubulin structure, they might compete for binding sites at growing microtubule plus ends. Competitive binding of SPR1 and *Arabidopsis* EB1b proteins to the microtubule lattice has been observed in microtubule cosedimentation assays (16). In addition, mutant analysis suggests that *SPR1* and *EB1b* have overlapping and sometimes antagonistic functions (16), consistent with SPR1 and EB1 competing for binding sites. SPR1 has been found to directly interact with EB1b (16); however, our data show that this interaction is not required for the plus end–tracking activity of SPR1. It remains to be determined whether binding of SPR1 and EB1b modulates their microtubule binding affinity and/or their ability to recruit other proteins to growing microtubule plus ends.

Previous work showed that the N- and C-terminal regions of SPR1 are individually not sufficient to bind to microtubules *in vivo* and do not rescue *spr1* mutants (11). However, N-GFP-C was partially functional and localized to microtubule plus ends *in vivo* (11). We found that both N-GFP-C and NC-GFP localize to growing microtubule plus ends *in vitro*, demonstrating that the N- and C-terminal regions, either separated or in tandem, are sufficient to target growing microtubule plus ends. These results also show that the spacing between the N- and C-terminal regions is not a critical determinant of SPR1's plus end–tracking activity, consistent with the high level of variability in amino acid sequence and length of the central region of SPR1 (11, 12).

Despite localizing to growing microtubule plus ends, both N-GFP-C and NC-GFP only partially complement the *spr1–6* mutant. The microtubule plus end binding affinity is about 2-fold lower for N-GFP-C and NC-GFP compared with full-length SPR1. In addition, although full-length SPR1 promotes microtubule dynamics, N-GFP-C and NC-GFP do not significantly affect microtubule dynamics. Together, these differences might explain why N-GFP-C and NC-GFP do not fully recapitulate SPR1 function *in vivo*.

The N-terminal GGG and C-terminal PGGG motifs of SPR1 have been proposed to mediate microtubule binding based on their similarity to the microtubule binding repeats of the MAP2/tau family of microtubule-associated proteins (16). However, MAP2/tau are not microtubule plus end–tracking proteins, and these repeat motifs contribute to their binding to the microtubule side walls, which primarily consist of GDP-state tubulin. We found that the N-terminal GGG motif is necessary for the +TIP activity of SPR1 and that the C-terminal PGGG motif enhances this activity. Elucidating how these motifs contribute to the binding of SPR1 to GDP/P_i-tubulin at growing microtubule plus ends will likely require structural information.

Live imaging of microtubule plus ends in animal cells is commonly conducted by exogenously expressing fluorescent protein–tagged EB1 or EB3 (20–24). However, because EB proteins form the core of microtubule plus-end complexes (25), their ectopic expression can potentially perturb endogenous microtubule plus-end complexes. Our finding that SPR1-GFP and NC-GFP label growing microtubule plus ends in HEK 293 cells demonstrates their utility as alternate +TIP markers in animal cells. Expression of SPR1-GFP in HEK293 cells slightly increased microtubule growth rates compared with control cells. In contrast, microtubules labeled by NC-GFP in HEK293 cells had only a minor increase in growth rate compared with control cells. Because NC-GFP minimally alters microtubule growth and is about half the size of SPR1 (~ 6 kDa), we propose NC-GFP as a versatile microtubule plus-end marker.

Experimental procedures

Constructs

For recombinant protein expression, a commercially synthesized SPR1-GFP construct was cloned into the pTEV plasmid between NcoI and XhoI restriction sites to obtain a C-terminal His_6 tag. The N-GFP-C construct was assembled using recombinant PCR. For this, EGFP was PCR-amplified with primers extending into the NSPR1 (5′-CAAAGCTCATTGGATTATCTCTTTGGTGGTGACGCTCCTATGGTGAGCAAGGGCGAG-3′) and CSPR1 regions (5′-TCCTTCAGCTCTGGCATAGTTGTTCTTGTACAGCTCGTCCATG-3′). Then CSPR1 was PCR-amplified with a forward primer containing 21 bp of the EGFP sequence (5′-GGCATGGACGAGCTGTACAAGAACAACTATGCCAGAGCTG-3′) and a reverse primer containing the XhoI restriction site (5′-TATCTCGAGCTTGCCACCAGTGAAGAGATAATCCAAGGATGATCCTCCTC-3′). These PCR fragments were then mixed at a 1:1 ratio and used as a template for a third PCR reaction with a forward primer consisting of the SPR1 N-terminal sequence and NcoI restriction site (5′-TATCCATGGGTCGTGGAAACAGCTGTGGTGGAGGT CAAAGCTCATTGGATTATC-3′) and a reverse primer containing the XhoI restriction site (5′-TATCTCGAGCTTGCCACCAGTGAAGAGATAATCCAAGGATGATCCTCCTC-3′). The resulting PCR product was inserted into the NcoI and XhoI sites of the pTEV plasmid. The NC-GFP construct was obtained by fusing the N- and C-terminal regions of SPR1 in a two-step PCR. The first PCR used primers 5′-CAAAGCTCATTGGATTATCTCTTTGGTGGTGACGCTCCTAACAACTATGCCAGAGCTGAAG-3′ and 5′-TATAGTCGACCTTGCCACCAGTGAAGAG-3′, and the second PCR used primers 5′-TATCCATGGGTCGTGGAAACAGC-

Figure 5. NC-GFP labels growing microtubule plus ends in animal cells. *A* and *B*, representative images of HEK293 cells expressing GFP-tubulin (*A*) or EB3-GFP (*B*). *Scale bar* = 5 μm. *C* and *D*, representative images of HEK293 cells expressing SPR1-GFP (*C*) or NC-GFP (*D*). *Scale bar* = 5 μm. *Numbers* in the images indicate time in seconds. *Arrowheads* point to examples of growing microtubule ends. *E*, dot plot of the microtubule growth rates in HEK293 cells expressing either GFP-tubulin, EB3-GFP, SPR1-GFP, or NC-GFP. ***, $p < 0.001$.

Downloaded from http://www.jbc.org/ at Washington University on November 1, 2019

TGTGGTGGAGGTCAAAGCTCATTGGATTATC-3′ and 5′-TATA GTCGACCTTGCCACCAGTGAAGAG-3′, with the first PCR product serving as a template. The resulting PCR product was inserted upstream of EGFP in the pTEV plasmid at NcoI and SalI sites. GGG-to-AAA and PGGG-to-AAAA mutant versions of SPR1 were generated using site-directed mutagenesis. The SPR1(Δ1–18)-GFP and SPR1(Δ87–119)-GFP truncation constructs were generated by replacing full-length SPR1 with PCR-amplified deletion fragments in the SPR1-GFP-His_6 construct.

To express *SPR1* under its native regulatory elements, we cloned a *SPR1* genomic fragment that included 896 bp upstream of the *SPR1* start codon using primers SPR1-attB1 (GGGGACAAGTTTGTACAAAAAAGCAGGCTGCGCCA-TTACACATGAATGGCCC) and SPR1-attB5r (GGGGACA-ACTTTTGTATACAAAGTTGTCTTGCCACCAGTGAA-GAGATAATC). This construct also included 700 bp down-stream of the *SPR1* stop codon that was amplified from genomic DNA using primers SPR1-attB4r (GGGGACAACTT-TTCTATACAAAGTTGCTTAAAATAATTGCAAAGACC-TTTATCTATCC) and SPR1-attB3r (GGGGACAACTTTAT-TATACAAAGTTGT AACACATTTGGAGCTGCATA-TGC). The EGFP coding sequence was inserted before the SPR1 stop codon. To express SPR1 under the *UBIQUITIN10* (*pUBQ10*) promoter, SPR1-GFP-His_6, N-GFP-C-His_6, and NC-GFP-His_6 were PCR-amplified using the respective bacterial expression vectors described above as templates and primers SPR1-attB5 (GGGGACAACTTTGTATACAAA-AGTTGCCGTCGACATGGGTCGTGGAAACAGCTG) and His_6-attB4 (GGGGACAACTTTGTATAGAAAAGT-TGGGTGGCGGCCGCTCAGTGGTGGTGGTGGTGGTG). All plant constructs were introduced in a pGAG binary vector containing a gentamycin-resistant cassette using gateway recombination. All constructs created using PCR were verified by sequencing.

Plant growth conditions

Plant constructs were transformed into the *spr1–6* mutant and an RFP-TUB6 microtubule marker line using an *Agrobacterium*-mediated floral dip method. To check the localization of SPR1-GFP in the *eb1a;eb1b* double mutant, p*SPR1:*g*SPR1-GFP* was transformed into an *eb1a;eb1b* line expressing the RFP-TUB6 marker. T1 seeds were surface-sterilized in 25% (v/v) bleach for 8 min, washed four to five times with sterile water, and suspended in 0.1% (w/v) agarose solution. Seeds were then plated on ½ MS plates containing 100 mg/liter gentamycin and stratified at 4 °C in dark for 3 days. To facilitate selection, stratified seeds were exposed to light for 6 h and then grown in the dark for 48 h at 23 °C, after which they were grown under long-day conditions (16 h light and 8 h dark) for another 48 h at 23 °C. For complementation experiments, at least 8 independent T1 lines were used to analyze the hypocotyl-skewing phenotype. Col-0 and *spr1–6* seedlings were used as controls and grown on ½ MS without gentamycin.

Protein purification

Escherichia coli Rosetta (DE3) cells were used for protein expression. Cells were grown to 0.6–0.8 A_{600} at 30 °C and then induced using 0.15 mM isopropyl 1-thio-β-D-galactopyranoside at 16 °C for 16–20 h. His_6-tagged proteins were isolated using nickel-nitrilotriacetic acid–agarose beads using lysis buffer (50 mM Tris (pH 8.0), 20 mM imidazole, 500 mM NaCl, 10% glycerol, 1% Tween 20, and protease inhibitors). Lysis buffer without Tween 20 and protease inhibitors was used for washing off unbound proteins, and wash buffer with 150 mM imidazole was used to elute protein from the nickel-nitrilotriacetic acid–agarose column. Purified proteins were desalted and exchanged into BRB80 buffer (80 mM piperazine-1,4-bis(2-ethanesulfonic acid), 1 mM $MgCl_2$, and 1 mM EGTA (pH 6.8)) supplemented with 10 mM DTT and 50 mM NaCl using PD-10 columns (GE Healthcare). Protein concentration was measured using the Bradford method. Proteins were aliquoted, snap-frozen in liquid nitrogen, and stored at −80 °C. All purified proteins used in this study had a His_6 tag attached at the C terminus of the protein.

Expression in animal cells

SPR1-GFP-His_6, N-GFP-C-His_6, and NC-GFP-His_6 were PCR-amplified using primers SPR1-SalI-EcoRI (TATAGTC-GACGAATTCATGGGTCGTGGAAACAGCTG) and His_6-SmaI (TATACCCGGGTCAGTGGTGGTGGTGGTGGTG) and the respective bacterial expression constructs described above as templates. The resulting PCR products were cloned into the EcoRI-SmaI restriction sites in the lentiviral vector pLVX-puromycin. The GFP-tubulin and EB3-GFP constructs were obtained from Weiping Han (Addgene plasmid 64060) (26) and the Washington University viral core facility, respectively. HEK293 cell transfection was conducted using 500 ng of DNA, and 2000 ng of polyethyleneimine HCl MAX (Polysciences, Inc.) was added to 50 μl of 300 mM NaCl. This solution was mixed, incubated for 10 min at room temperature, and then added to the plated cells in culture medium containing 10% fetal bovine serum in DMEM plus 1% penicillin-streptomycin. Cells were imaged 24–48 h after transfection. Expression in HEK293 cells was repeated four times. Quantification of microtubule growth rate was repeated twice (n = 20 cells for SPR1-GFP, n = 32 cells for NC-GFP, n = at least 10 cells each for EB3-GFP and GFP-tubulin).

Total internal reflection fluorescence microscopy

For the *in vitro* reconstitution assays, flow chambers were prepared by attaching silanized coverslips to a glass slide using two layers of double-sided adhesive tape. GMPCPP-stabilized (Jena Biosciences) microtubule seeds were prepared by polymerizing 50 μM porcine tubulin containing biotin-labeled (1:14.5) and rhodamine-labeled (1:14.5) porcine tubulins (Cytoskeleton, Inc.) in the presence of 1 mM GMPCPP at 37 °C for 30 min. The polymerized microtubules were then collected by centrifugation at 25,000 × g for 20 min, resuspended in 50 μl of warm BRB80 containing 1 μM GMPCPP, and fragmented by passing through a 100-μl Hamilton syringe four to five times. Flow chambers were first coated with 20% anti-biotin antibody (Sigma-Aldrich), followed by blocking with 5% Pluronic for 5 min each. Then 300 nM GMPCPP-stabilized seeds were added and allowed to bind to the anti-biotin antibody for 5 min. Microtubule polymerization was initiated by adding a mixture of 20 μM

Downloaded from http://www.jbc.org/ at Washington University on November 1, 2019

1:25 rhodamine-labeled porcine tubulin (*i.e.* 4% of the tubulin is rhodamine-labeled), 1% methylcellulose (4000 cP, Sigma-Aldrich), 50 mM DTT, 2 mM GTP, an oxygen-scavenging system (250 mg/ml glucose oxidase, 35 mg/ml catalase, and 4.5 mg/ml glucose), and different concentrations of SPR1 or mutant proteins, as indicated in the text. 5-mW 488-nm and 5-mW 561-nm diode-pumped, solid-state lasers were used to excite GFP and rhodamine, respectively. Images were collected by a ×100 (numerical aperture 1.45) objective with a 2x tube lens and a back-illuminated electron-multiplying charge-coupled device camera (ImageEM, Hamamatsu) at 2.5-s intervals and for a total of about 5 min.

For single-molecule imaging experiments, we used 100 nM, 150 nM, and 250 nM of SPR1-GFP, NC-GFP, and N-GFP-C proteins, respectively. Images were captured at 10 frames/s in streaming mode. A snapshot of microtubules was taken just before and immediately after the streaming mode acquisition to document microtubule growth. For photobleaching experiments, we used 1 nM of SPR1-GFP, NC-GFP, and N-GFP-C proteins. To promote photobleaching, we exited GFP using 20 mW of laser power. Images were acquired at an exposure time of 100 ms and 200-ms intervals between frames.

For GTPγS microtubule binding experiments, we followed the method described in Maurer *et al.* (4). Flow chambers with GMPCPP microtubule seeds bound to anti-biotin antibody on coverslips were prepared as described above. Microtubule polymerization was initiated by adding a polymerization mixture as described above with the following modifications: 25 μM porcine tubulin (4% of which is rhodamine-labeled), 10 mM 2-mercaptoethanol, and 2 mM GTPγS (Sigma) with 500 nM SPR1-GFP or NC-GFP.

Live imaging of *Arabidopsis* seedlings was done using 4-day-old T1 seedlings. At least three independent T1 lines were used for these experiments. Live imaging of HEK293 cells was conducted 2–3 days after transfection. Specimens were illuminated with 3-mW 488-nm and 3-mW 561-nm lasers to excite GFP and RFP, respectively.

Data analysis

Microtubule dynamics and single-molecule kinetics were quantified from kymographs of individual microtubules generated using the Fiji ImageJ package (27). Microtubule growth and shortening rates were calculated for individual growth and shortening phases. Rescue frequency was calculated by dividing the sum of the number of transitions from shrinkage to growth by the time spent shrinking. Catastrophe frequency was calculated by dividing the sum of the number of transitions from growth to shrinkage by the time spent growing. To determine the microtubule transition frequency, a switch from growth to shortening or vice versa was considered as a transition event. When a microtubule depolymerized all the way back to the GMPCPP seed followed by a pause of 5 or more frames, subsequent microtubule growth was considered as an independent microtubule growth event and not a transition event of the previous microtubule. SPR1-GFP signal intensity plots were created using the plot profile tool in Fiji. The angles of hypocotyl cell files were measured with respect to the hypocotyl growth axis using the angle measure tool in Fiji. Dot plots and statistical analyses were conducted using GraphPad Prism. All data points were included in the statistical analyses.

Author contributions—R. B., L. F., V. C., and R. D. conceptualization; R. B., L. F., R. E., and R. D. formal analysis; R. B., L. F., E. E., and R. E. investigation; R. B., L. F., E. E., and R. E. visualization; R. B., L. F., and E. E. methodology; R. B. writing-original draft; R. B., L. F., E. E., R. E., V. C., and R. D. writing-review and editing; V. C. and R. D. supervision; V. C. and R. D. funding acquisition; V. C. and R. D. project administration.

Acknowledgments—We thank Marcus Mahar and Dianne Duncan for help with the animal cell experiments, Rashmi Nanjundappa and Moe Mahjoub for providing the pLVX-puromycin plasmid, Weiping Han for providing the L304-EGFP-tubulin construct, and Takashi Hashimoto for providing the eb1a;eb1b double-mutant line.

References

1. Akhmanova, A., and Steinmetz, M. O. (2010) Microtubule +TIPs at a glance. *J. Cell Sci.* **123,** 3415–3419 CrossRef Medline
2. Bieling, P., Laan, L., Schek, H., Munteanu, E. L., Sandblad, L., Dogterom, M., Brunner, D., and Surrey, T. (2007) Reconstitution of a microtubule plus-end tracking system *in vitro*. *Nature* **450,** 1100–1105 CrossRef Medline
3. Dixit, R., Barnett, B., Lazarus, J. E., Tokito, M., Goldman, Y. E., and Holzbaur, E. L. (2009) Microtubule plus-end tracking by CLIP-170 requires EB1. *Proc. Natl. Acad. Sci. U.S.A.* **106,** 492–497 CrossRef Medline
4. Maurer, S. P., Bieling, P., Cope, J., Hoenger, A., and Surrey, T. (2011) GTPγS microtubules mimic the growing microtubule end structure recognized by end-binding proteins (EBs). *Proc. Natl. Acad. Sci. U.S.A.* **108,** 3988–3993 CrossRef Medline
5. Maurer, S. P., Fourniol, F. J., Bohner, G., Moores, C. A., and Surrey, T. (2012) EBs recognize a nucleotide-dependent structural cap at growing microtubule ends. *Cell* **149,** 371–382 CrossRef Medline
6. Maurer, S. P., Cade, N. I., Bohner, G., Gustafsson, N., Boutant, E., and Surrey, T. (2014) EB1 accelerates two conformational transitions important for microtubule maturation and dynamics. *Curr. Biol.* **24,** 372–384 CrossRef Medline
7. Roth, D., Fitton, B. P., Chmel, N. P., Wasiluk, N., and Straube, A. (2018) Spatial positioning of EB family proteins at microtubule tips involves distinct nucleotide-dependent binding properties. *J. Cell Sci.* **132,** jcs219550 Medline
8. Honnappa, S., Gouveia, S. M., Weisbrich, A., Damberger, F. F., Bhavesh, N. S., Jawhari, H., Grigoriev, I., van Rijssel, F. J., Buey, R. M., Lawera, A., Jelesarov, I., Winkler, F. K., Wüthrich, K., Akhmanova, A., and Steinmetz, M. O. (2009) An EB1-binding motif acts as a microtubule tip localization signal. *Cell* **138,** 366–376 CrossRef Medline
9. Kumar, A., Manatschal, C., Rai, A., Grigoriev, I., Degen, M. S., Jaussi, R., Kretzschmar, I., Prota, A. E., Volkmer, R., Kammerer, R. A., Akhmanova, A., and Steinmetz, M. O. (2017) Short linear sequence motif LxxPTPh targets diverse proteins to growing microtubule ends. *Structure* **25,** 924–932.e4 CrossRef Medline
10. Wong, J. H., and Hashimoto, T. (2017) Novel *Arabidopsis* microtubule-associated proteins track growing microtubule plus ends. *BMC Plant Biol.* **17,** 33 CrossRef Medline
11. Nakajima, K., Furutani, I., Tachimoto, H., Matsubara, H., and Hashimoto, T. (2004) SPIRAL1 encodes a plant-specific microtubule-localized protein required for directional control of rapidly expanding *Arabidopsis* cells. *Plant Cell* **16,** 1178–1190 CrossRef Medline
12. Sedbrook, J. C., Ehrhardt, D. W., Fisher, S. E., Scheible, W. R., and Somerville, C. R. (2004) The *Arabidopsis* sku6/spiral1 gene encodes a plus end-localized microtubule-interacting protein involved in directional cell expansion. *Plant Cell* **16,** 1506–1520 CrossRef Medline

Downloaded from http://www.jbc.org/ at Washington University on November 1, 2019

13. Young, R. E., and Bisgrove, S. R. (2011) in *The Plant Cytoskeleton* (Liu, B. ed.) pp. 95–117, Springer, New York, NY
14. Furutani, I., Watanabe, Y., Prieto, R., Masukawa, M., Suzuki, K., Naoi, K., Thitamadee, S., Shikanai, T., and Hashimoto, T. (2000) The SPIRAL genes are required for directional control of cell elongation in *Arabidopsis thaliana*. *Development* **127,** 4443–4453 Medline
15. Nakajima, K., Kawamura, T., and Hashimoto, T. (2006) Role of the SPIRAL1 gene family in anisotropic growth of *Arabidopsis thaliana*. *Plant Cell Physiol.* **47,** 513–522 CrossRef Medline
16. Galva, C., Kirik, V., Lindeboom, J. J., Kaloriti, D., Rancour, D. M., Hussey, P. J., Bednarek, S. Y., Ehrhardt, D. W., and Sedbrook, J. C. (2014) The microtubule plus-end tracking proteins SPR1 and EB1b interact to maintain polar cell elongation and directional organ growth in *Arabidopsis*. *Plant Cell* **26,** 4409–4425 CrossRef Medline
17. Dixit, R., Chang, E., and Cyr, R. (2006) Establishment of polarity during organization of the acentrosomal plant cortical microtubule array. *Mol. Biol. Cell* **17,** 1298–1305 CrossRef Medline
18. Komaki, S., Abe, T., Coutuer, S., Inzé, D., Russinova, E., and Hashimoto, T. (2010) Nuclear-localized subtype of end-binding 1 protein regulates spindle organization in *Arabidopsis*. *J. Cell Sci.* **123,** 451–459 CrossRef Medline
19. Lindeboom, J. J., Nakamura, M., Saltini, M., Hibbel, A., Walia, A., Ketelaar, T., Emons, A. M. C., Sedbrook, J. C., Kirik, V., Mulder, B. M., and Ehrhardt, D. W. (2018) CLASP stabilization of plus ends created by severing promotes microtubule creation and reorientation. *J. Cell Biol.* **218,** 190–205 CrossRef Medline
20. Yang, C., Wu, J., de Heus, C., Grigoriev, I., Liv, N., Yao, Y., Smal, I., Meijering, E., Klumperman, J., Qi, R. Z., and Akhmanova, A. (2017) EB1 and EB3 regulate microtubule minus end organization and Golgi morphology. *J. Cell Biol.* **216,** 3179–3198 CrossRef Medline
21. Mimori-Kiyosue, Y., Shiina, N., and Tsukita, S. (2000) The dynamic behavior of the APC-binding protein EB1 on the distal ends of microtubules. *Curr. Biol.* **10,** 865–868 CrossRef Medline
22. Ma, Y., Shakiryanova, D., Vardya, I., and Popov, S. V. (2004) Quantitative analysis of microtubule transport in growing nerve processes. *Curr. Biol.* **14,** 725–730 CrossRef Medline
23. Salaycik, K. J., Fagerstrom, C. J., Murthy, K., Tulu, U. S., and Wadsworth, P. (2005) Quantification of microtubule nucleation, growth and dynamics in wound-edge cells. *J. Cell Sci.* **118,** 4113–4122 CrossRef Medline
24. Stepanova, T., Slemmer, J., Hoogenraad, C. C., Lansbergen, G., Dortland, B., De Zeeuw, C. I., Grosveld, F., van Cappellen, G., Akhmanova, A., and Galjart, N. (2003) Visualization of microtubule growth in cultured neurons via the use of EB3-GFP (end-binding protein 3-green fluorescent protein). *J. Neurosci.* **23,** 2655–2664 CrossRef Medline
25. Lansbergen, G., and Akhmanova, A. (2006) Microtubule plus end: a hub of cellular activities. *Traffic* **7,** 499–507 CrossRef Medline
26. Yang, W., Guo, X., Thein, S., Xu, F., Sugii, S., Baas, P. W., Radda, G. K., and Han, W. (2013) Regulation of adipogenesis by cytoskeleton remodelling is facilitated by acetyltransferase MEC-17-dependent acetylation of α-tubulin. *Biochem. J.* **449,** 605–612 CrossRef Medline
27. Schindelin, J., Arganda-Carreras, I., Frise, E., Kaynig, V., Longair, M., Pietzsch, T., Preibisch, S., Rueden, C., Saalfeld, S., Schmid, B., Tinevez, J. Y., White, D. J., Hartenstein, V., Eliceiri, K., Tomancak, P., and Cardona, A. (2012) Fiji: an open-source platform for biological-image analysis. *Nat. Methods* **9,** 676–682 CrossRef Medline

Downloaded from http://www.jbc.org/ at Washington University on November 1, 2019

ASBMB

Mechanism of microtubule plus-end tracking by the plant-specific SPR1 protein and its development as a versatile plus-end marker

Rachappa Balkunde, Layla Foroughi, Eric Ewan, Ryan Emenecker, Valeria Cavalli and Ram Dixit

J. Biol. Chem. 2019, 294:16374-16384.
doi: 10.1074/jbc.RA119.008866 originally published online September 16, 2019

Access the most updated version of this article at doi: 10.1074/jbc.RA119.008866

Alerts:
- When this article is cited
- When a correction for this article is posted

Click here to choose from all of JBC's e-mail alerts

This article cites 26 references, 15 of which can be accessed free at
http://www.jbc.org/content/294/44/16374.full.html#ref-list-1

Downloaded from http://www.jbc.org/ at Washington University on November 1, 2019